Clays and Clay Minerals, Vol. 59, No. 2, 165–175, 2011.

IN SITU X-RAY DIFFRACTION STUDY OF THE SWELLING OF MONTMORILLONITE AS AFFECTED BY EXCHANGEABLE CATIONS AND TEMPERATURE

SHOJI MORODOME† AND KATSUYUKI KAWAMURA*,‡

Department of Earth and Planetary Science, Tokyo Institute of Technology, Ookayama 2-12-1, Megro-ku, Tokyo 152-8551, Japan

Abstract—The swelling property of smectite is dominated by the hydration of exchangeable cations in the interlayer spacing ('interlayer hydration'). By investigating systematically the swelling behavior of various exchangeable cations with different valences and ionic radii, the interlayer hydration of smectite was explored. The swelling behavior of Li^+-, K^+-, Rb^+-, Cs^+-, Mg^{2+}-, Sr^{2+}-, Ba^{2+}-, and La^{3+}-montmorillonites in undersaturated conditions was measured precisely over the range 50−150ºC by *in situ* X-ray diffraction (XRD) analyses. The systematic swelling behavior of ten homocationic montmorillonites, the aforementioned eight homoionic montmorillonites, plus Na^+ and Ca^{2+} from a previous study, and the cation hydration energies were analysed by studying the changes occurring in the basal spacing and the 001 peak width. With decreasing cation hydration energy, swelling curves (*i.e*. plots of basal spacing *vs.* relative humidity (RH)) change from continuous (Mg^{2+}, La^{3+}, and Ca^{2+}) to stepwise (Sr^{2+}, Li^+, Ba^{2+}, and Na^+) to one-layer only (K^+, Rb^+, and Cs^+). For the first two groups, the RH at the midpoint between the one- and two-layer hydration states increased as the cation hydration energy decreased. Under low RH, with increasing temperature, the basal spacings of Mg-, La-, Ca-, Sr-, Li-, and Ba-montmorillonites decreased continuously to the zero-layer hydration state, whereas Na-, K-, Rb-, and Cs-montmorillonites swelled from the zero-layer hydration state even at the lowest temperature (50ºC). A decrease in the basal spacing at the same RH but at different temperatures suggests the existence of metastable states or that the layer-stacking structure changes with temperature. The systematics of the swelling behavior of various homocationic montmorillonites as functions of RH and temperature (<150ºC) at 1 atm are reported here.

Key Words—Basal Spacing, Hydration, Interlayer Exchangeable Cation, Montmorillonite, Relative Humidity, Smectite, Swelling, Vapor Pressure, X-ray Diffraction.

INTRODUCTION

Smectite is known to exhibit a distinct swelling behavior with respect to the layer charge and the exchangeable cations present in its interlayer spacing. Other than smectite, few inorganic minerals exhibit such behavior; cation hydration in the micro-interlayer spacing is unusual. In order to understand the nature of cation hydration, investigation of the interlayer hydration of smectite is essential. This is important not only for pure materials science but also for potential engineering applications such as the behavior of the exchangeable cation hydration and two-dimensional interlayer water solutions.

* E-mail address of corresponding author:
kats@cc.okayama-u.ac.jp
Present addresses:
† Research Laboratories, Kunimine Industries Co. Ltd., Nabekake 1085-454, Nasushiobara, Tochigi 325-0013, Japan
‡ Graduate School of Environmental Science, Okayama University, 3-1-1, Tsushimanaka, Kita-Ku, Okayama, Okayama 700-8530, Japan
DOI: 10.1346/CCMN.2011.0590205

The swelling behavior of undersaturated smectite has been reported by various investigators since the 1950s (Table 1), including *in situ* changes in XRD spacings of Wyoming and Tsukinuno montmorillonites, both well known, naturally occurring montmorillonites. The change in swelling behavior as a function of the exchangeable cation (Na^+, K^+, and Ca^{2+}) for Wyoming montmorillonite (Berend *et al*., 1995; Cases *et al*., 1997; Ferrage *et al*., 2005a) was almost identical to that of the Tsukinuno montmorillonite (Watanabe and Sato, 1988; Sato *et al*., 1992), in spite of their different mineral locality, composition, and layer charge. Ferrage *et al*. (2005a, 2005b, 2007) performed XRD-profile modeling of 00*l* reflections as a way to analyze swelling behavior. They found good agreement between the experimental patterns and those obtained using their model and interpreted the results in terms of the heterogeneity of smectite hydration (the existence of mixed-layer hydration), change in interlayer distance, coherent scattering domain size, distribution of interlayer water *vs*. RH, exchangeable cation, and value and location of the layer charge. Using this technique they found a small amount of the two-molecular-layer hydration state for K-montmorillonite. In addition, a trend for the swelling behavior *vs.* the ionic radii and the valence of the exchangeable

Table 1. Previous observations for swelling behavior of smectite with various exchangeable cations.

Specimen	Exchangeable cation	Layer charge, z (e)	Method	Reference
Wyoming montmorillonite (Volclay)	H^+, Na^+, Cs^+, Ca^{2+}, Ba^{2+}	Unknown	Quenched	Mooney *et al*. (1952)
Kozakov saponite Czech Republic $E_{0.455}[Mg_{2.50}Fe^{2+}_{0.26}Fe^{3+}_{0.24}][Si_{3.30}Al_{0.68}Fe^{3+}_{0.02}]O_{10}(OH)_2$	Li^+, Na^+, K^+, Mg^{2+}, Ca^{2+}, Ba^{2+}	0.455	Quenched	Suquet *et al*. (1975)
Hectorite, California $E_{0.29}[Mg_{2.71}Li_{0.29}][Si_4]O_{10}(F,OH)_2$	Li^+, Na^+, K^+, Cs^+, Mg^{2+}, Ca^{2+}, Sr^{2+}, Ba^{2+}	0.29	*In situ*	Prost (1975)
Tsukinuno montmorillonite (T1) Saponite, Ballarat, California (SapCa-1)	Na^+, K^+, Ca^{2+}	0.40(T1) 0.38 (SapCa-1)	*In situ*	Watanabe and Sato (1988)
Two Tsukinuno montmorillonites (TU6) Tetrahedral E = 0.24 Octahedral E = 0.16 (Ts) Tetrahedral E = 0.07 Octahedral E = 0.39	Na^+, K^+, Ca^{2+}	0.4(TU6) 0.46(Ts)	*In situ*	Sato *et al*. (1992)
Wyoming montmorillonite $E_{0.380}[Al_{1.530}Mg_{0.257}Fe^{2+}_{0.006}Fe^{3+}_{0.207}][Si_{3.883}Al_{0.117}]O_{10}(OH)_2$	Li^+, Na^+, K^+, Rb^{2+}, Cs^+, Mg^{2+}, Ca^{2+}, Sr^{2+}, Ba^{2+}	0.38	*In situ*	Berend *et al*. (1995) Cases *et al*. (1997)
Synthetic smectite Na:Mg:Al:Si = 0.5:1.1:3.0:8.0	Li^+, Na^+, K^+, Mg^{2+}, Ca^{2+}	~0.25	*In situ*	Tamura *et al*. (2000)
Wyoming montmorillonite $E_{0.35}[Al_{1.495}Fe_{0.215}Mg_{0.26}][Si_{3.985}Al_{0.015}]O_{10}(OH)_2$	Li^+, Na^+, K^+, Mg^{2+}, Ca^{2+}, Sr^{2+}	0.35	*In situ*	Ferrage *et al*. (2005)
Tsukinuno montmorillonite $E_{0.564}[Al_{1.56}Mg_{0.31}Fe^{2+}_{0.01}Fe^{3+}_{0.09}][Si_{3.91}Al_{0.09}]O_{10}(OH)_2$	Na^+, Ca^{2+}	0.564	*In situ*	Morodome and Kawamura (2009)

cation was revealed. For naturally occurring montmorillonites, this change may be summarized as follows: in K-, Rb-, and Cs-montmorillonites, the two-molecular-layer hydration state is scarcely visible. The basal spacing of the Li- and Na-montmorillonites under low-RH conditions decreased with increasing cationic radius. In the montmorillonite with divalent cations, the RH at which the basal spacing reaches the two-molecular-layer hydration states increased with increasing cationic radius.

Hectorite exhibited a different behavior (Prost, 1975) from montmorillonite. For K-hectorite, the swelling curve reached the two-molecular-layer hydration state at the lowest RH condition. In hectorite with divalent cations, the RH at which the basal spacing reached the two-molecular-layer hydration state was not correlated to the cationic radius. The swelling curves of these hectorites did not increase continuously, but had inflection points for the Mg- and Ca-exchanged forms. Unlike naturally occurring smectite, the swelling behavior of well crystallized synthetic smectite (Nakazawa *et al*., 1992) exhibited a distinct stepwise hydration as a function of RH (Tamura *et al*., 2000). The full-width at half-maximum (FWHM) of the 001 reflection was extremely small compared with that of naturally occurring smectites. In the synthetic smectite, the RH at which the basal spacing reached the two-molecular-layer hydration state increased with increasing ionic radius for the same valence cations; for the K-smectite, the two-layer hydration state was not observed. The swelling behavior in terms of the exchangeable cations is essentially the same as that of naturally occurring montmorillonites, except for step or continuous changes.

In all these *in situ* studies, the swelling behavior was measured at RH intervals of ~10% and only at room temperature. In order to investigate the effects of temperature on the swelling properties, Morodome and Kawamura (2009) observed the swelling behavior of the Na- and Ca-Tukinuno montmorillonite at various temperatures ranging over 50−150ºC using *in situ* XRD. The XRD measurements were performed at small RH intervals in order to understand the swelling behavior precisely.

The purpose of the present study was to conduct a careful investigation of the swelling properties of eight homoionic montmorillonites, including mono-, di-, and trivalent cations (Li^+, K^+, Rb^+, Cs^+, Mg^{2+}, Sr^{2+}, Ba^{2+}, and La^{3+}), at temperatures ranging over 50−150ºC using environmental *in situ* XRD measurements; and to investigate the differences in the swelling behavior in

https://doi.org/10.1346/CCMN.2011.0590205 Published online by Cambridge University Press

terms of exchangeable cations at various temperatures, together with those of the Na- and Ca-montmorillonite (Morodome and Kawamura, 2009).

EXPERIMENT

Sample preparation

The material used was montmorillonite obtained from the Tsukinuno Mine, in Yamagata prefecture, Japan (Kunipia-F, Kunimine Industry Co. Ltd., Japan), the same as that used by Morodome and Kawamura (2009). The structural formula of the montmorillonite was reported to be $Na_{0.42}Ca_{0.068}K_{0.008}[Si_{3.91}Al_{0.09}](Al_{1.56}Mg_{0.31}Fe(III)_{0.09}Fe(II)_{0.01})O_{10}(OH)_2$ (Ito *et al.*, 1993). The layer charge of this high-charge montmorillonite was calculated to be 0.564 e^- per formula unit and the cation exchange capacity (CEC) is 116 meq/100 g (Ito *et al.*, 1993). In order to obtain mono-cationic Li-, K-, Rb-, Cs-, Mg-, Sr-, Ba-, and La-montmorillonites, ion-exchange experiments were conducted as follows: the montmorillonites were dispersed in metal chloride aqueous solutions (1 eq/L), followed by centrifugation in a CN-2060 instrument (Hsiangtai Machinery Ind. Co., Taipei, China) (12 min, 4000 rpm, $1800 \times g$), washing with pure water (>1 MOhm-cm), and finally drying at 100ºC, the same procedure as that of Morodome and Kawamura (2009). Following oven drying, the montmorillonite samples were not ground but were mixed with water in an agate mortar. The cation contents were checked semi-quantitatively by scanning electron microscopy and energy dispersive spectroscopy (SEM-EDS). For XRD measurements, the montmorillonite sample was mixed with water in an agate mortar, smeared onto a ceramic tile (10 mm × 20 mm), and dried at room temperature.

X-ray measurements

The procedure for the XRD experiments was the same as that for Morodome and Kawamura (2009). A θ-θ type X-ray diffractometer (Rint-Ultima III, Rigaku Co., Ltd., CuKα radiation) and an environmental sample chamber in which the temperature and humidity were controlled precisely were used. The sample temperature was set at 50, 70, 90, 110, 130, and 150ºC. The RH in the sample chamber was varied from extra dry to nearly saturated conditions at a sample temperature of <100ºC, or to P_{H_2O} = ~0.1 MPa at sample temperatures >100ºC (Table 2). The scanning range was 2−12º2θ at a scan rate of 0.5º2θ min^{-1}, for all sample temperatures. Wide-angle measurements (2−34º2θ) were made for each sample to observe higher 00l peaks. Repeated measurements were performed for each RH and temperature condition until the diffraction pattern ceased to change. The typical number of repeats was 2 or 3; and a minimum of 3 h up to a maximum of 12 h was required to attain a stable state. Polarization, absorption, and base-line corrections were made to the 001 peak in order to obtain the basal spacing and peak width. The 001 peak of smectite is often broad and asymmetric. The maximum intensity of the 001 peak was measured in the present study using quadratic interpolation of three adjacent points at intervals of 0.05º, including the maximum-intensity point. The peak width is equivalent to the FWHM. Uncorrected diffraction data are displayed in all figures.

RESULTS AND DISCUSSION

Swelling behavior of montmorillonite with monovalent exchangeable cations

A series of XRD patterns was plotted *vs.* the RH for Li- and K-montmorillonites at 70ºC (Figures 1a and 1b, respectively). The d_{001} and the peak width were plotted *vs.* RH for the Li-, K-, Rb-, and Cs-montmorillonite (Figures 2a and 2b, respectively).

The 001 peak of the Li-montmorillonite showed almost no change at the one-layer hydration state from RH = 3.0% to 50.5% at 70ºC (Figure 1a). For RH = 3.0%, a peak at ~14.7º2θ was observed, which is assigned to the 002 peak of the one-molecular-layer hydration state, and is denoted below as 002_{1L}, following the notation of Morodome and Kawamura (2009). From RH = 3.0% to 50.5%, the 002_{1L} peak intensity decreased gradually, and the position of the peak moved slightly to the lower-angle side, which was different from the case of the Na-montmorillonite. A broad 001 peak appeared at the transition state from RH = 55.6% to 58.2%, where the 002_{1L} peak intensity was very low. For RH values in the range 67.0%−95.8%, the 001 peak shifted gradually to the lower-angle side at the

Table 2. The extra dry conditions and the conditions with greatest humidity depend on the temperature in the sample chamber of the X-ray diffractometer, because for the water-vapor generator temperature = 6ºC, P_{H_2O} = 0.93 kPa, and up to 94ºC, P_{H_2O} = 81.47 kPa) (Morodome and Kawamura, 2009).

Sample temperature	50ºC	70ºC	90ºC	110ºC	130ºC	150ºC
Water-vapor generator temperature	Min 6ºC Max 49ºC	Min 6ºC Max 69ºC	Min 6ºC Max 89ºC	Min 6ºC Max 94ºC	Min 6ºC Max 94ºC	Min 6ºC Max 94ºC
Relative humidity	Min 7.5% Max 95.1%	Min 3.0% Max 95.8%	Min 1.3% Max 96.2%	Min 0.6% Max 56.9%	Min 0.3% Max 30.2%	Min 0.2% Max 17.1%

https://doi.org/10.1346/CCMN.2011.0590205 Published online by Cambridge University Press

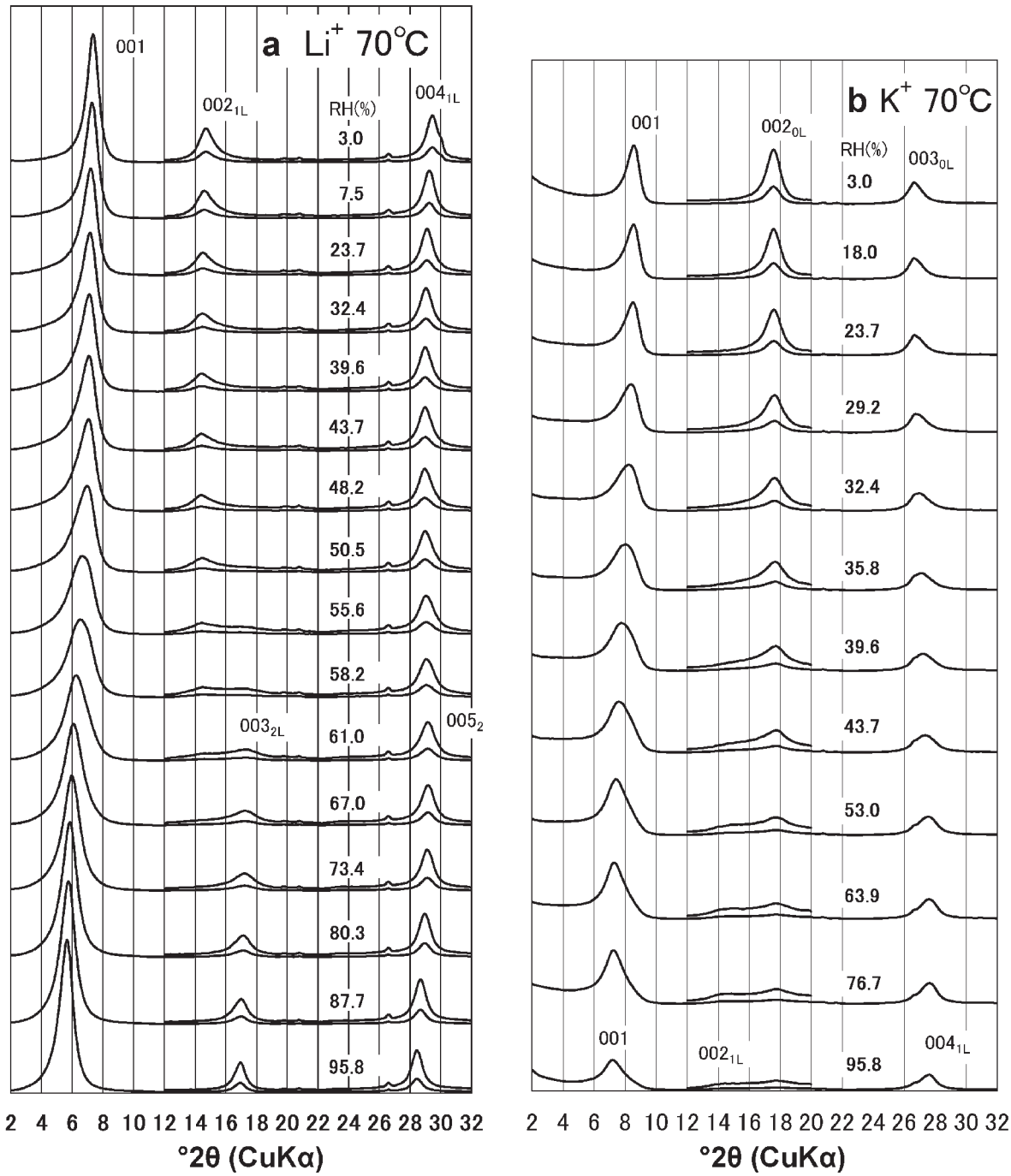

Figure 1. XRD profiles of (a) Li- and (b) K-montmorillonite from 2 to 32º2θ under various RH conditions and at 70ºC. The intensity scale of this part of the profiles was expanded by a factor of three.

two-layer hydration state. Under these conditions, the 003_{2L} peak intensity increased gradually, and the peak shifted slightly toward the lower-angle side. The 004_{1L} peak also shifted slightly toward the lower-angle side from RH = 3.0% to 48.2%. For RH values in the range 48.2%–61.0%, the peak shifted to the higher-angle side; moreover, the peak was replaced by the 005_{2L} peak because the 004_{1L} and 005_{2L} peaks overlapped each other under these conditions, which were the same as those for the Na-montmorillonite. For RH values in the range 61.0–95.8%, the 005_{2L} peak shifted slightly to the lower-angle side.

The 001 peak of the K-montmorillonite changed continuously from 8.4º2θ (RH = 3.0%) to 7.2º2θ (95.8%)

https://doi.org/10.1346/CCMN.2011.0590205 Published online by Cambridge University Press

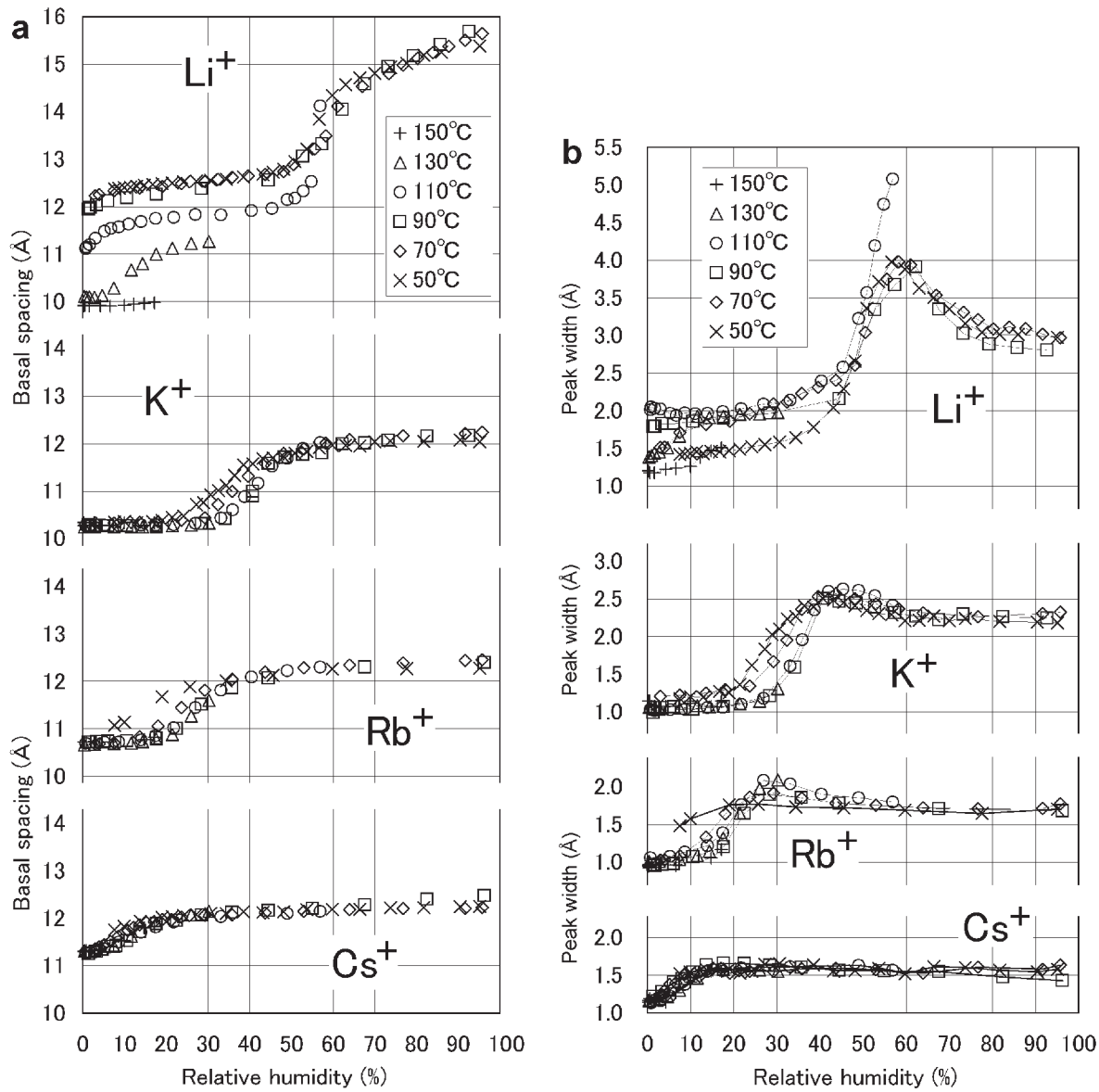

Figure 2. Change in (a) the basal spacing and (b) the peak width of Li-, K-, Rb-, and Cs-montmorillonite from 50 to 150ºC.

at 70ºC (Figure 1b). Under these conditions, the 002_{0L} peak intensity decreased gradually and the peak position was almost unchanged with increasing RH, which is same as that observed for the Na-montmorillonite. The 002_{1L} peak intensity at 14.2º2θ increased gradually from RH = 53.0% to 95.8%. Because the 003_{0L} peak position (26.6º2θ) was close to that of the 004_{1L} peak position (27.5º2θ), and these peaks overlapped each other; with increasing RH, the 003_{0L} peak shifted to the higher-angle side and was replaced by the 004_{1L} peak. The XRD pattern profiles of the Rb- and Cs-montmorillonite *vs.* RH behaved almost identically to those of the K-montmorillonite.

With increasing temperature, the basal spacing of the Li-montmorillonite at low RH decreased gradually from the one-layer to the zero-layer hydration state (Figure 2a). At 150ºC, only the zero-layer hydration state was observed (d_{001} = ~9.9 Å) from RH = 0.3% to 17.1%. The basal spacing increased gradually from the extra-dry condition to the one-layer hydration state with increasing RH, which is different from what is seen with Na-montmorillonite. These differences are attributed to the large hydration energy of the Li^+ ion as compared with that of the Na^+ ion. At temperatures >90ºC, the basal spacing of the one-layer hydration state decreased from ~12.4 to 11.1 Å with increasing temperature. From 50 to

https://doi.org/10.1346/CCMN.2011.0590205 Published online by Cambridge University Press

90ºC, the basal spacing changed gradually, then at 110ºC it changed abruptly from the one-layer to the two-layer hydration state. The RH at which the transition occurred between the one- and the two-layer hydration states (~55%) shifted slightly with temperature, and was less than that of the Na-montmorillonite (~72%). The peak width of the Li-montmorillonite was not a maximum at the transition between the zero-layer and one-layer hydration states at temperatures between 110 and 130ºC (Figure 2b), which is different from the case of the Na-montmorillonite. Between the one-layer and two-layer hydration states, the peak width was a maximum for each temperature. In such transformation regions, at least two different domains of mixed-layer stacking are suggested. At 110ºC, the maximum peak width was larger (~5.1 Å) than that from 50 to 90ºC (~4.0 Å). With increasing RH, the basal spacing of the two-layer hydration state of the Li-montmorillonite increased from ~14.5 to 15.6 Å (Figure 2a) compared to the relatively small increase in that of the Na-montmorillonite (~15.0 to 15.6 Å).

At all temperatures, the basal spacing of the K-, Rb-, and Cs-montmorillonite swelled up to that of the one-

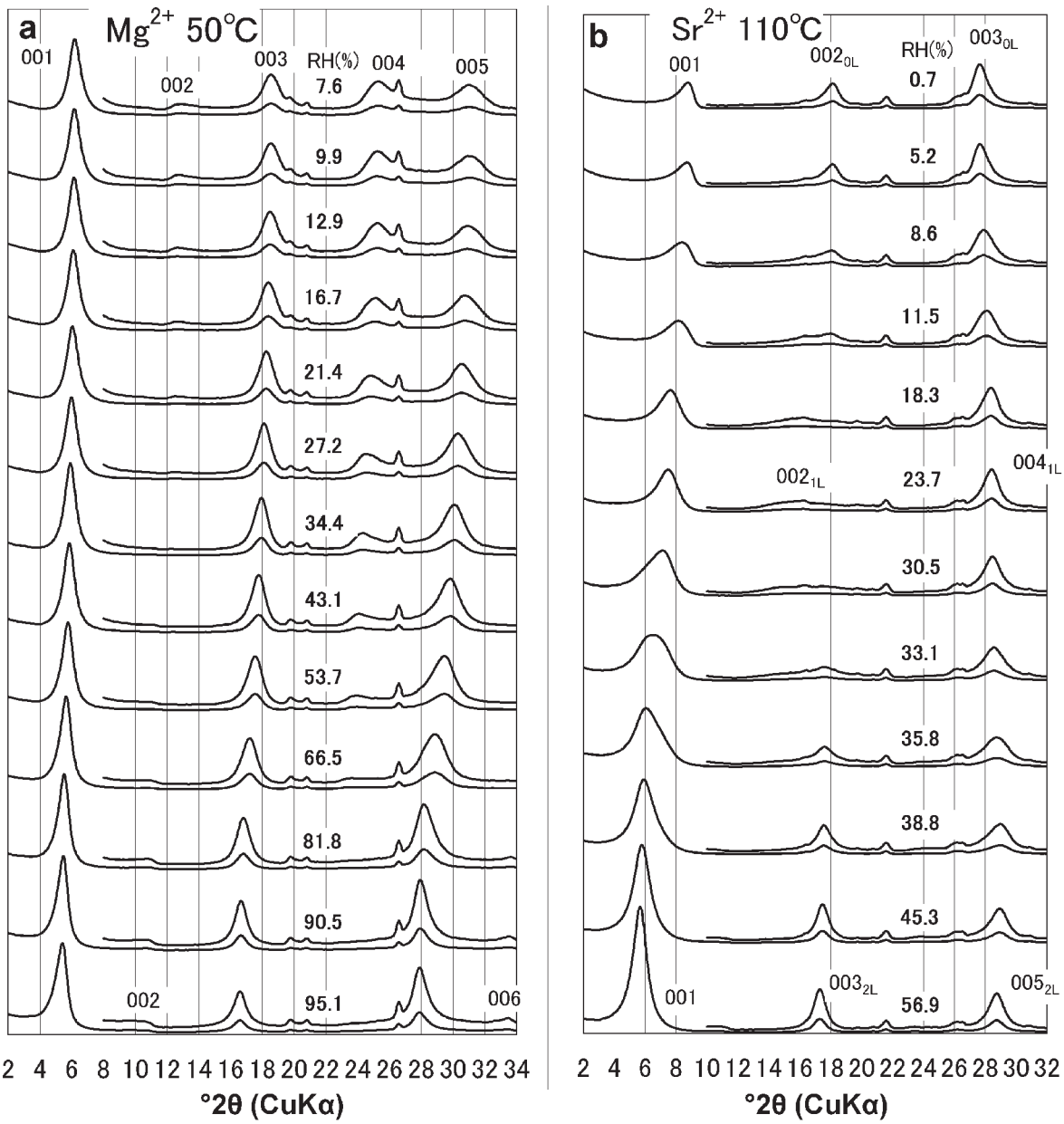

Figure 3. XRD profiles of (a) Mg-montmorillonite from 2 to 34º2θ and (b) Sr-montmorillonite from 2 to 32º2θ under various RH conditions and at 50ºC (Mg) or 110ºC (Sr). The intensity scale of this part of the profiles was expanded by a factor of three.

https://doi.org/10.1346/CCMN.2011.0590205 Published online by Cambridge University Press

layer hydration state, and the two-layer hydration state was not observed, even for very high RH conditions (~95%, see Figure 2a). The basal spacings at the lowest RH conditions were 10.2, 10.8, and 11.2 Å for the K-, Rb-, and Cs-montmorillonite, respectively (Figure 2a). The d values of the 002_{0L} peak (17.6º2θ, 5.0 Å) and 003_{0L} peak (26.6º2θ, 3.4 Å) at the lowest RH conditions for the K-montmorillonite were about one-half and one-third of the d_{001} value (10.2 Å), respectively (Figure 1b). These peaks are considered to be of a rational series, and probably represent a zero-layer hydration state or a slightly mixed-layer hydration state (0w/1w); the d_{001} value was larger than that of Li-montmorillonite (9.9 Å), however. The same applied to Rb-montmorillonite (d_{001} = 10.8 Å, d_{002} = 5.2 Å, d_{003} = 3.4 Å) and Cs-montmorillonite (d_{001} = 11.2 Å, d_{001} = 5.5 Å, d_{001} = 3.5 Å). The basal spacing of the zero-layer hydration state increased systematically with increasing ionic radius. With increasing RH, the basal spacing increased gradually from the zero-layer to the one-layer hydration state. The Cs-montmorillonite reached the one-layer hydration state at the lowest RH (~20%), followed by the

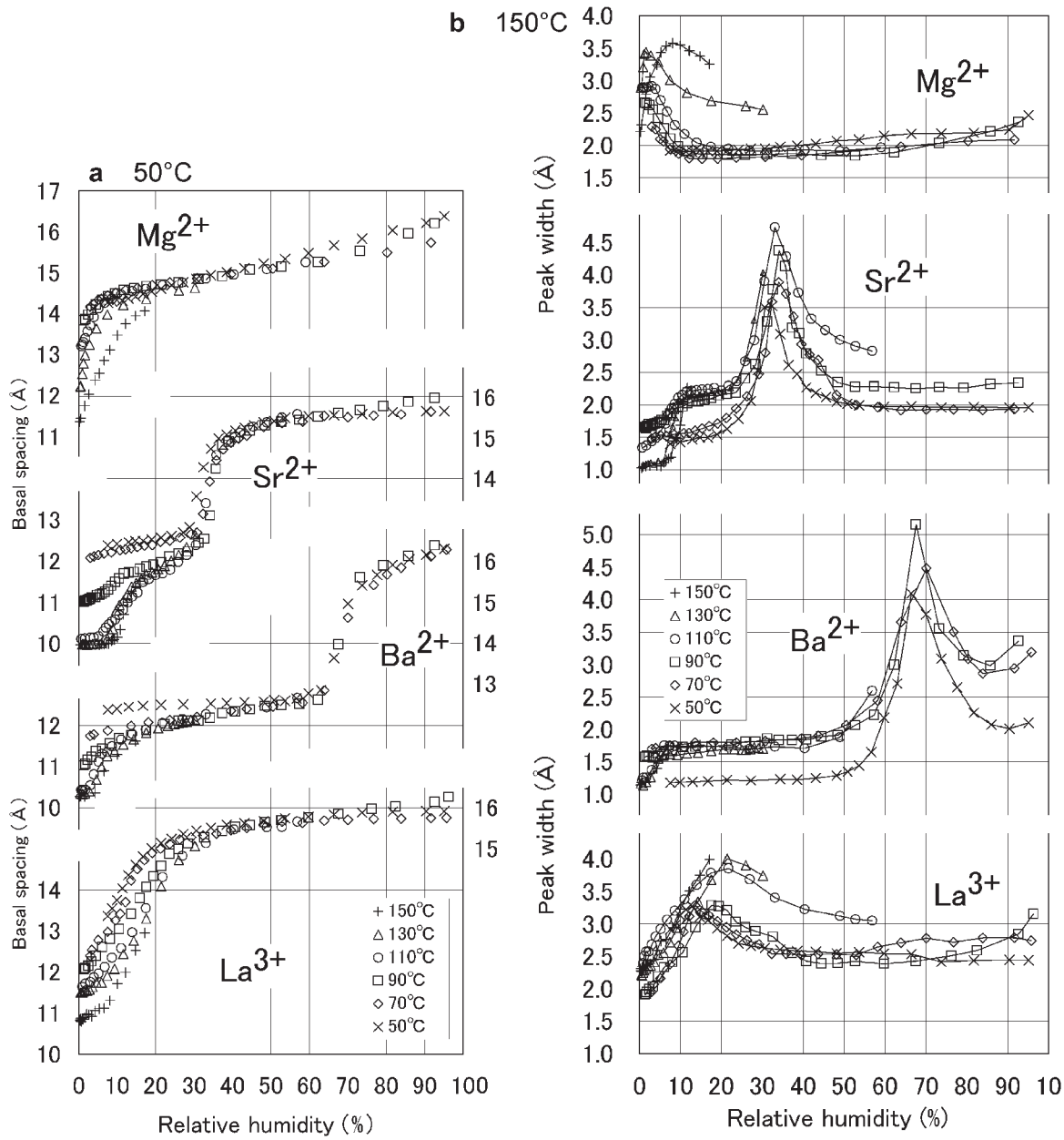

Figure 4. Changes in (a) the basal spacing and (b) the peak width of Mg-, Ca-, Sr-, Ba-, and La-montmorillonite from 50 to 150ºC.

https://doi.org/10.1346/CCMN.2011.0590205 Published online by Cambridge University Press

Rb- (~35%) and K-montmorillonites (~45%). The swelling curves of the K-, Rb-, and Cs-montmorillonites between the zero-layer and one-layer hydration states shifted slightly toward greater RH with increasing temperature (Figure 2a), the same result as noted for the Na-montmorillonite. Between the zero-layer and one-layer hydration states, the peak width was greatest in the K-, Rb-, and Cs-montmorillonites (Figure 2b). The maximum peak width was K- (~2.5 Å) > Rb- (~2.0 Å) > Cs-montmorillonite (~1.6 Å). The basal spacing for the one-layer hydration state was almost the same for the K-, Rb-, and Cs-montmorillonites (~12.2 Å, see Figure 2a).

Swelling behavior of montmorillonite with di- and trivalent exchangeable cations

A series of XRD profiles at various RH for the Mg- and Sr-montmorillonites at 50ºC and 110ºC (Figures 3a and 3b, respectively) were examined; the d_{001} values and the peak width *vs.* RH for the Mg-, Sr-, Ba-, and La-montmorillonites were plotted. (Figures 4a and 4b, respectively). The position of the 001 peak of the Mg-montmorillonite decreased gradually from 6.2º2θ (RH = 7.6%) to 5.4º2θ (95.1%) at 50ºC (Figure 3a). Under these conditions, the higher-angle peaks also shifted to the lower-angle side with increasing RH, which is the same as for Ca-montmorillonite. The XRD profiles *vs.* RH of the La-montmorillonite behaved essentially the same as that of the Mg-montmorillonite.

The position of the 001 peak of the Sr-montmorillonite decreased from 8.7º2θ (RH = 0.7%) to 7.5º2θ (23.7%) at 110ºC (Figure 3b). Under these conditions, the 002_{0L} peak intensity decreased gradually and the peak shifted slightly toward the lower-angle side with increasing RH. A broad 001 peak was observed from RH = 30.5% to 35.8%. The intensity of the 002_{1L} peak is very small under these conditions. From RH = 38.8% to 56.9%, the 001 peak intensity increased gradually and the peak position decreased slightly. The intensity of the 003_{2L} peak increased gradually, and the peak position decreased slightly under such conditions. Because the peaks of 003_{0L} (27.7º2θ), 004_{1L} (28.3º2θ), and 005_{2L} (29.0º2θ) overlap each other from 0.7% to 45.3%, the 003_{0L} peak replaced the 004_{1L} peak, and the 004_{1L} peak replaced the 005_{2L} peak. The 005_{2L} peak shifted slightly toward the lower-angle side from 45.3% to 56.9% RH. The XRD profiles acquired at various RH in the Ba-montmorillonite behaved essentially the same as those of the Sr-montmorillonite.

The basal spacing of Mg- and La-montmorillonite increased continuously to the two-layer hydration state for all temperatures (Figure 4a), which is same as that for the Ca-montmorillonite. With increasing temperature, the basal spacing of these montmorillonites at lower RH conditions decreased gradually to the basal spacing of the zero-layer hydration state (Figure 4a). The Mg-montmorillonite reached the two-layer hydration state at low RH (~8%) compared to the La-montmorillonite (RH ~25%, see Figure 4a). With increasing RH, the relative increase in the basal spacing of the two-layer hydration state of the Mg-montmorillonite (~14.5−16.0 Å) was larger than that of the La-montmorillonite (~15.5−16.0 Å, see Figure 4a). Both the maximum peak width and the RH at the transition state of the Mg- and La-montmorillonites increased gradually with increasing temperature (Figure 4b), although these values for the Mg-montmorillonite were smaller than those of the La-montmorillonite.

The results for the swelling of the Sr- and Ba-montmorillonites revealed clearly the zero-, one-, and two-layer hydration states and the two transition states (Figure 4a). With increasing temperature, the basal spacing of the Sr- and Ba-montmorillonites under extra-dry conditions (Table 2) decreased continuously, from the one-layer to the zero-layer hydration state (Figure 4a). Above 110ºC, the basal spacing of the Ba-montmorillonite under extra-dry conditions was designated as corresponding to the zero-layer hydration state (Figure 4a). The spacing (10.2 Å) is larger than that

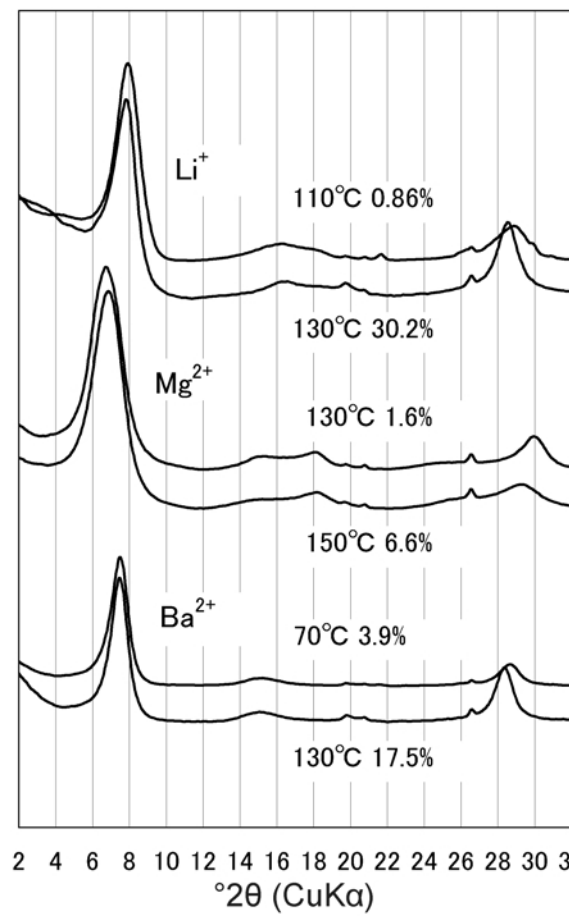

Figure 5. Comparison of two diffraction profiles of the same basal spacing at different temperatures for Li-, Mg-, and Ba-montmorillonite.

https://doi.org/10.1346/CCMN.2011.0590205 Published online by Cambridge University Press

of the typical zero-layer hydration state because of the large ionic radius of the Ba^{2+} ion, as noted also for the K-, Rb-, and Cs-montmorillonites. With increasing RH, the basal spacing of the Sr- and Ba-montmorillonites increased gradually from the extra-dry state to the one-layer hydration state and, for lower RH, the swelling curve declined with increasing temperature (Figure 4a). The basal spacing of the Ba-montmorillonite reached that of the one-layer hydration state at ~9% RH, which was less than that of the Sr-montmorillonite (~13%). The peak width of the samples increased gradually from the extra-dry state to the one-layer hydration state with increasing RH, and did not exhibit a maximum under these conditions (Figure 4b). The RH of the transition state between the one-layer and two-layer hydration states shifted with temperature between the Sr- (~30%) and Ba- (~70%) montmorillonites (Figure 4a). Between the one-layer and two-layer hydration states, the peak width exhibited a maximum, and the peak width increased gradually with increasing temperature for these samples (Figure 4b). The peak width of the Sr-montmorillonite was smaller than that of the Ba-montmorillonite. With increasing RH, the basal spacing of the two-layer hydration state increased from 15.2 to 15.8 Å for the Sr-montmorillonite, and from 15.6 to 16.1 Å for the Ba-montmorillonite (Figure 4a).

The basal spacing at low RH conditions (from the zero-layer to one-layer hydration states) decreased gradually with increasing temperature for montmorillonites with divalent cations, La^{3+}, and Li^{+} (Figures 2a, 4a). However, the basal spacing of these montmorillonites was almost unchanged with temperature at greater

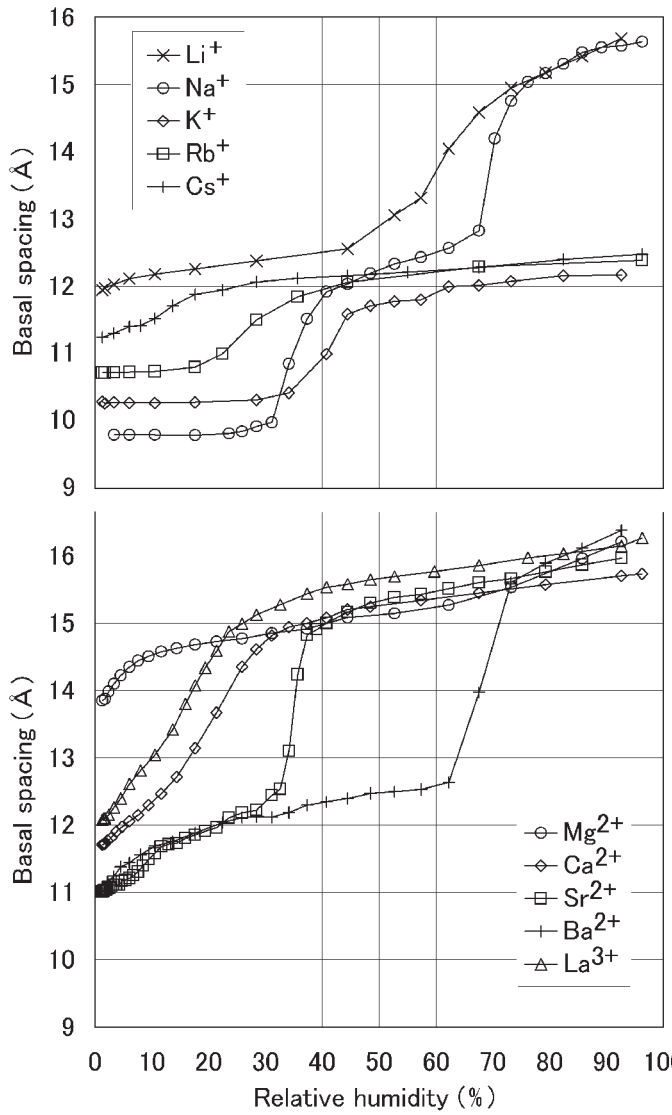

Figure 6. Changes in basal spacings for nine homocationic montmorillonites at 90ºC.

https://doi.org/10.1346/CCMN.2011.0590205 Published online by Cambridge University Press

RH conditions in going from the one-layer to the two-layer hydration states.

For the Li-, Mg-, and Ba-montmorillonites, the two diffraction profiles exhibiting the same basal spacing at different temperatures were compared (Figure 5). In the XRD profiles, the angle and intensity of peaks at ~16º2θ and 29º2θ for these montmorillonites differed from each other (Figure 5), indicating that the layer-stacking structure depends on temperature in spite of having the same basal spacings. These measurements were carried out after the sample was dried for ~24 h at a temperature >10ºC above the sample temperature and under extremely dry conditions. These different characteristics of the XRD profiles suggest the existence of metastable states or a layer-stacking structure that changes as a function of temperature.

SWELLING BEHAVIOR *VS.* HYDRATION ENERGY OF THE EXCHANGEABLE CATION

Plots of d_{001} *vs.* RH for the Li-, K-, Rb-, Cs-, Mg-, Sr-, Ba-, and La-montmorillonites at 90ºC, together with the d_{001} values for the Na- and Ca-montmorillonites taken from Morodome and Kawamura (2009) (Figure 6) revealed that, under dry conditions, the basal spacing was ~9.8 Å, the one-layer hydration spacing was 12.1−12.5 Å, and the two-layer hydration spacing was 14.6−16.2 Å (Figure 6).

The swelling behavior of the various exchangeable cations can be categorized into three types: (1) Cs^+, Rb^+, K^+: swelling only up to the one-layer hydration state; (2) Na^+, Ba^{2+}, Li^+, Sr^{2+}: stepwise swelling to the one-layer and two-layer hydration states; and (3) Ca^{2+}, La^{3+}, Mg^{2+}: continuous swelling to the two-layer hydration state. The hydration energy of these exchangeable cations is proportional to the ratio of their valence to ionic radii (Shannon, 1976):

$$Cs^+ < Rb^+ < K^+ < Na^+ < Ba^{2+} \leqslant Li^+ < Sr^{2+} < Ca^{2+} < La^{3+} < Mg^{2+}$$

The RH of the mid-point of the transition between the one-layer and two-layer hydration states, RH_{1-2}, increased systematically with decreasing hydration energy except for the K-, Rb-, and Cs-montmorillonites, which only swelled to the one-layer hydration state (Figure 7). The RH_{1-2} was determined by the RH of the maximum peak width observed at the transition state between the one-layer and two-layer hydration states. Such phenomena were only revealed by observations at high temperatures.

At the lowest temperature, 50ºC, the swelling curves in the present study were almost the same as those obtained in studies of Wyoming montmorillonite at about room temperature (Berend *et al*., 1995 [30ºC]; Cases *et al*., 1997 [30ºC]; Ferrage *et al*., 2005a [24ºC]). The Wyoming montmorillonite (z = 0.35−0.38) has a low layer charge compared with the Tsukinuno montmorillonite (z = 0.40−0.564), however. Although, differences are apparent between the hectorite (Prost, 1975) and montmorillonite, the layer charge of hectorite (z = 0.29) is similar to that of Wyoming montmorillonite. K-hectorite swells to the two-layer hydration state. The value of RH_{1-2} for the K-hectorite is the smallest among the monovalent exchangeable cations, and the difference between the swelling properties of the hectorite and of the materials studied in the present work is insignificant

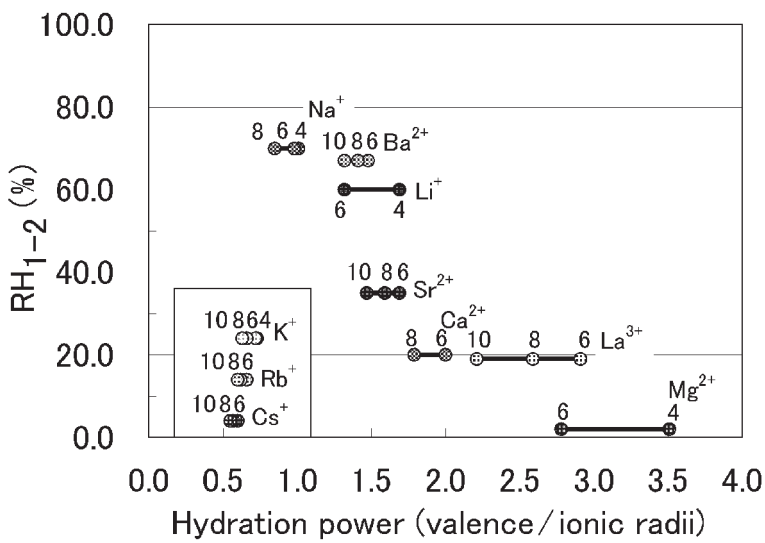

Figure 7. Relation between the hydration energy (ionic valence/ionic radius) and the RH_{1-2} of the mid point of transition between one- and two-layer hydration states at 90ºC. The number above each closed circle shows the coordination number of the cation. Because the basal spacing of K-, Rb-, and Cs-montmorillonite indicated swelling only up to the one-layer hydration state, only the hydration energy is shown.

https://doi.org/10.1346/CCMN.2011.0590205 Published online by Cambridge University Press

in terms of the value of RH_{1-2} for the various divalent cations.

CONCLUSIONS

The swelling behavior of the montmorillonite with various homo-ionic cations (Li^+, K^+, Rb^+, Cs^+, Mg^{2+}, Sr^{2+}, Ba^{2+}, and La^{3+}) was observed by *in situ* XRD measurements at various temperatures up to 150ºC, and at RHs below 100% (where the RH was varied with small intervals). The swelling behavior for various exchangeable cations was classified into three types depending on the hydration energy of the cations; with decreasing cation hydration energies, swelling curves changed from continuous (Mg^{2+}, La^{3+}, and Ca^{2+}) to stepwise (Sr^{2+}, Li^+, Ba^{2+}, and Na^+) to one-layer only (K^+, Rb^+, and Cs^+). Additional study is required to understand the change in the swelling curve *vs.* temperature at low-RH conditions for the montmorillonite with divalent exchangeable cations, La^{3+}, and Li^+ because the swelling curves at each temperature did not coincide even under the same RH conditions. The Tsukinuno and Wyoming montmorillonites showed almost the same swelling characteristics, whereas hectorite behavior differed from these. Systematic studies of the swelling behavior of various other smectite minerals are needed to further understand the essential features of smectite swelling. Detailed discussion of the swelling behavior based on these experiments alone would be inappropriate. In order to analyze the swelling behavior from a physicochemical view point (as done by Ferrage *et al*., 2005a, 2005b, 2007), XRD-pattern simulation, in which patterns are calculated by the stacking sequence of some one-dimensional clay-unit models, will be performed in a future study.

ACKNOWLEDGMENTS

The work here was supported partly by KAKENHI (19540501 and 21540493). The authors thank Drs Masashi Nakano, Yasuaki Ichikawa, Masahiro Shibata, Haruo Sato, and Satoru Suzuki for helpful discussions.

REFERENCES

Berend, I., Cases, J.M., Francois, M., Uriot, J.P., Michot, L., Maison, A., and Thomas, F. (1995) Mechanism of adsorption and desorption of water vapor by homoionic montmorillonites: 2. the Li^+, Na^+, K^+, Rb^+ and Cs^+-exchanged forms. *Clays and Clay Minerals*, **43**, 324–336.

Cases, J.M., Berend, I., Francois, M., Uriot, J.P., Michot, L.J., and Thomas, F. (1997) Mechanism of adsorption and desorption of water vapor by homoionic montmorillonites: 3. the Mg^{2+}, Ca^{2+}, Sr^{2+} and Ba^{2+}-exchanged forms. *Clays and Clay Minerals*, **45**, 8–22.

Ferrage, E., Lanson, B., Sakharov, B.A., and Drits, V.A. (2005a) Investigation of smectite hydration properties by modeling experimental X-ray diffraction patterns. Part I. Montmorillonite hydration properties. *American Mineralogist*, **90**, 1358–1374.

Ferrage, E., Lanson, B., Malikova, N., Plançon, A., Sakharov, B.A., and Drits, V.A. (2005b) New insights on the distribution of interlayer water in bi-hydrated smectite from X-ray diffraction profile modeling of 00*l* reflections. *Chemistry of Materials*, **17**, 3499–3512.

Ferrage, E., Lanson, B., Sakharov, B.A., Geoffroy, N., Jacquot, E., and Drits, V.A. (2007) Investigation of dioctahedral smectite hydration properties by modeling of X-ray diffraction profiles: Influence of layer charge and charge location. *American Mineralogist*, **92**, 1731–1743.

Ito, M., Okamoto, M., Shibata, M., Sasaki, Y., Danbara, T., Suzuki, K., and Watanabe, T. (1993) Mineral composition analysis of bentonite. PNC TN8430 93-003, Japan Atomic Energy Agency. (in Japanese).

Mooney, R.W., Keenan, A.G., and Wood, L.A. (1952) Adsorption of water vapor by montmorilllonite. II. Effect of exchangeable ions and lattice swelling as measured by X-ray diffraction. *Journal of the American Chemical Society*, **74**, 1371–1374.

Morodome, S. and Kawamura, K. (2009) Swelling behavior of Na- and Ca-montmorillonite up to 150ºC by *in situ* X-ray diffraction experiments. *Clays and Clay Minerals*, **57**, 150–160.

Nakazawa, H., Yamada, H., and Fujita, T. (1992) Crystal synthesis of smectite applying very high pressure and temperature. *Applied Clay Science*, **6**, 395–401.

Prost, R. (1975) Étude de l'hydratation des argiles: Interactions eau-minéral et mécanisme de la rétention de l'eau. II. Étude d'une smectite (hectorite). *Annales Agronomiques*, **26**, 463–535.

Sato, T., Watanabe, T., and Otsuka, R. (1992) Effects of layer charge, charge location, and energy change on expansion properties of dioctahedral smectites. *Clays and Clay Minerals*, **40**, 103–113.

Shannon, R.D. (1976) Revised effective ionic radii and systematic studies of interatomic distances in halides and chalcogenides. *Acta Crystallographica Section A*, **32**, 751–767.

Suquet, H., De La Calle, C., and Pezerat, H. (1975) Swelling and structural organization of saponite. *Clays and Clay Minerals*, **34**, 379–384.

Tamura, K., Yamada, H., and Nakazawa, H. (2000) Stepwise hydration of high-quality synthetic smectite with various cations. *Clays and Clay Minerals*, **48**, 400–404.

Watanabe, T. and Sato, T. (1988) Expansion characteristics of montmorillonite and saponite under various relative humidity conditions. *Clay Science*, **7**, 129–138.

(*Received 2 July 2010; revised 21 April 2011; Ms. 453; A.E. R. Dohrmann*)